Extraction of Squilla (*Harpiosquilla annandalei*) shell derived chitosan and its nanocarrier efficiency for sustained protein delivery

Akshad Balde[1] , Bhavika Waghela[1] , Nazeer Rasool Abdul[1,*]

[1]Biopharmaceuticals Lab, Department of Biotechnology, School of Bioengineering, SRM Institute of Science and Technology, Kattankulathur-603203, Chennai, Tamilnadu, India

*Corresponding author
Nazeer Rasool Abdul, PhD
Biopharmaceuticals Lab
Department of Biotechnology,
School of Bioengineering, SRM
Institute of Science and Technology,
Kattankulathur, Chennai 603 203,
Tamilnadu, India
e-mail: nazeerr@srmist.edu.in

ABSTRACT

The delivery of proteins has enormous potential in chronic disease treatment and immunomodulation. But, because of the intrinsic properties of proteins such as poor stability and quick bio clearance, their usage is limited in targeted delivery. This work suggests a cost-effective method to prepare an efficient polymer-based nanocarrier system for the sustained delivery of protein. Herein, low molecular weight chitosan (CS) was extracted from the shell waste of squilla (*Harpiosquilla annandalei*) (sCS) and characterized. It showed higher water-binding capacity (WBC) of 548 ± 11.7% as well as fat binding capacity (FBC) of 369 ± 19.9% respectively, as compared to commercial CS (cCS). BSA loaded nanoparticles were synthesized through the ionic gelation method using cCS and sCS. The **s**CS-based BSA encapsulated nanoparticles (BSA-sCSNPs) were observed to be uniform and small (60-195 nm) as compared to BSA loaded cCS-based nanoparticles (BSA-cCSNPs). The encapsulation efficiency (EE%) was highest for 1 mg/mL CS, BSA, and tripolyphosphate (TPP) based BSA-sCSNPs. Moreover, the *in vitro* BSA release profile exhibited that BSA-sCSNPs resulted in more stable and sustained release till the 16th h (85.4 ± 1.15%) than BSA-cCSNPs. Further, the sCS and BSA-sCSNPs were biocompatible with L929 cells and showed no cytotoxic effects. Thus, this biocompatible nanoparticle system can be used as a pharmaceutical as well as a nutraceutical agent to improve the stability as well as targeted delivery of the protein.

INTRODUCTION

Nanomaterials are of great significance over conventional formulations due to their ability to release drugs in a controlled manner, extended diffusion time, and targeted delivery with reduced side effects. Recent progress made in this field has opened paths for expanding the clinical value of nanomaterials in several sectors, including agriculture for developing nano fertilizers, the medicinal field for tissue regeneration and cancer therapy, as well as emerging biomedical engineering for the development of a drug with the least toxic effects in a continuous way [1-2]. Further advancements have led to the synthesis of efficient nanocarrier systems for anti-microbial, anti-cancerous, and anti-inflammatory drug delivery [3-6]. The delivery of proteins has enormous potential in chronic disease treatment, immunomodulation, and various therapeutic applications [2]. But, because of the intrinsic properties of proteins such as poor stability and quick bio clearance, their usage is limited in targeted delivery and hence, protein-nanoparticle systems can protect the target protein from enzymatic degradation and renal clearance [7]. Previous studies by Scaletti et al. [8] reported several protein delivery carriers that have shown reduced toxic effects and efficient cellular uptake. Moreover, delivery of proteins through a polymer-based nanocarrier system is

observed to show enhanced functionalization, targeting ability, and prolonged circulation time. Proteins conjugated with polymers using crosslinkers develop a supramolecular structure that maintains the integrity and intrinsic properties of the protein throughout the delivery process into the cells. The protein delivery studies through marine-based polymeric Nano systems are limited and need further exploration for enhanced diffusion efficacy and release rate.

Many products such as peptides, proteins, bioactive compounds, and polymers extracted from oceanic animals have shown a spectrum of bioactivity and pharmacological properties that can be extracted from animal parts like scales, vestigial organs, tissues, and exoskeletons as well [9-12]. Furthermore, marine crustaceans such as crabs, shrimps, and squilla are widely used to extract polymers like CS, alginate, collagen, and gelatin as these natural polymers show high bioavailability, low toxicity, and biodegradability as compared to chemically synthesized polymers [13-15]. The CS is the most abundant biomaterial available and is mainly used for the preparation of nanomaterials due to its low molecular weight, mucoadhesive, and availability of multiple administration ways. Furthermore, because of their nanometric scale, these nanoparticles can overcome the tissue barriers in the human body and can reach a specific site to increase the plasma clearance of the drug [16]. Many studies have revealed that low molecular weight CS can show enhanced nanocarrier efficiency and prevail sustained drug release, which may be due to the cationic nature of CS in an acidic environment, as most of the polysaccharides are negatively charged or neutral [17].

H. annandalei is a crustacean found in the Indian Ocean that belongs to the Malacostraca class and family Squillidae. Crustacean fish processing is increasing due to the high nutritional content of crab and shrimp tissues. Nevertheless, the shells and exoskeletons are discarded near the harbor, leading to oceanic pollution [18]. Hence, these shells can be used to produce industrially, and pharmaceutically beneficial products used in numerous applications [19]. Although, as far as we know, no previous research has investigated biological applications of *H. annandalei* shell-derived CS in the field of protein delivery. Moreover, research findings for the enhancement of CS nanocarrier efficiency are also limited, and hence, there is a need to investigate the parameters for the development of an effective protein-CS nanocarrier for sustained delivery. Therefore, in the present study, sCS was used to develop BSA-sCSNPs using the ionic gelation method. These nanoparticles were characterized and compared with BSA-cCSNPs for their nanocarrier efficiency. Moreover, the *in vitro* release profile of BSA from nanoparticles was also explored in detail using the dialysis method to analyze the effect of different CS, BSA, and TPP concentrations. Furthermore, the cytotoxic effects of cCS, sCS, BSA-cCSNPs, and BSA-sCSNPs were studied on L929 cells at different concentrations.

MATERIALS AND METHODS

Materials

The *H. annandalei* was collected from the fish landing trash of the Royapurum sea coast (13. 6' 26" N, 80"7'43" E), Tamilnadu, India. The shells were washed, and the tissue content was removed and then stored at -20°C for further use. BSA, cCS (Degree of deacetylation (DD); >85% and MW; 150-310 kDa), TPP (Molecular weight: 367.86 g/mol), and Whatman filter paper No. 1 were acquired from Sigma-Aldrich (St. Louis, MO, USA). Dialysis Membrane-60 (1.5 cm diameter; 1.9 ml/cm capacity) was procured

from HiMedia Laboratories Pvt. Ltd. (Mumbai, India). Moreover, analytical grade source chemicals and deionized water were used in all studies.

Proximate analysis

The total protein in the crude sample was calibrated according to Lowry et al. [20]. Further, the total moisture content present in the sample was determined by weighing the shells before and after sun drying in the pre-weighed aluminium dish (to obtain a constant mass, the samples were dried in the oven at 105°C). Ash content was estimated by charging the pre-dried sample in a crucible at 6000°C and weighing the remains. Furthermore, the sulfuric acid method described by Albalasmeh et al. [21] was used for the estimation of carbohydrate content using UV absorbance at 315 nm.

Extraction and purification of CS from squilla shells

Dried squilla shells were pulverized and chitin was extracted using three different steps (deproteinization, demineralization, and decolorization) as described by Rao et al. [22]. Initially, protein and sugars were dissolved through the deproteinization step by treating shells with 4% NaOH for 2 h at 30°C and filtration using Whatman filter paper to acquire residue. Further, the residue was subjected to the demineralization step for the removal of minerals, mainly calcium carbonate, which was achieved by mixing the residue with 4% HCl at 30°C with continuous stirring for 12 h and further filtration using Whatman filter paper. The obtained residues after both steps were subjected to protein and ash content analysis. Furthermore, astaxanthins and pigments were removed to yield a cream-white powder using 0.315% NaOCl bleaching for 5 minutes at 37°C followed by filtration and drying at 60°C to obtain powdered chitin. Further, the chitin was converted to CS using the deacetylation step, which involves the treatment of chitin with 50% NaOH and constant stirring at 65°C for 18 h on the hot plate. The extracted CS was oven-dried at 120°C for 24 h and purified using 2% acetic acid in 1 N NaOH followed by filtration to remove insoluble particles.

Preparation of BSA-CSNPs using the ionic gelation method

The purified CS was further used for the preparation of BSA-loaded CSNPs based on the ionic gelation of cationic CS with anionic TPP [23]. CS solutions were prepared with different concentrations (3-1 mg/mL) by dissolving CS into a desired proportion of acetic acid. Further, BSA with different concentrations (3–1 mg/mL) was added into the CS solution and the TPP solution (0.5–1.5 mg/mL) with a 4:1 ratio was added using a syringe filter where the solution was stirred simultaneously for 1 h using a magnetic stirrer until the opalescent suspension was observed. Subsequently, the suspension was centrifuged, and the pellets were subjected to freeze-drying at -20°C. A series of BSA-CSNPs were prepared with different concentrations of CS, BSA, and TPP to study effects on EE%.

Characterization of CS and developed nanoparticles

The functional group peaks of cCS, sCS, BSA-cCSNPs, and BSA-sCSNPs were recorded on the Perkin-Elmer Fourier-transform infrared (FTIR) spectrometer (Cary Agilent 600 series, Victoria, Australia) within the resolution of 4 cm-1 and the frequency range of 400–4000 cm-1. Further, X-ray diffraction (XRD) peak measurement was done through

XPERT-PRO XRD, and the analysis was performed using a Diffractometer system (BRUKER D8 Advance, Davinci, USA) with CuKa radiation Λ = 1.54060 [A], 45 kV, 40 mA, and scan step time 2[s] for studying the physical nature and crystallinity index (CrI) of samples [24]. Further, *scanning electron microscope* (SEM) imaging was carried out on JSM-5600LV (JEOL, Tokyo, Japan) equipped with energy dispersive X-ray analysis (EDAX) at an acceleration voltage of 20 kV to analyze the surface morphology and presence of heavy metal elements in the extracted CS. Further, the size distribution and zeta potential of BSA-cCSNPs and BSA-sCSNPs were analyzed using photon correlation spectroscopy and laser Doppler anemometry [25]. The analysis was performed at 25°C with a detection angle of 90°.

Physicochemical property analysis of CS and developed nanoparticles

The DD% was determined for CS samples through the obtained FTIR peaks at a frequency of 1655 cm^{-1} and 3450 cm^{-1}. Further, the average molecular weight and viscosity of CS were determined by a viscometer (Viscologic Ti 1 SEMAtech). 0.2 M acetic acid and 0.1 M sodium acetate were used for the dissolution of CS powder followed by filtration through a 0.22 μm Millipore membrane, and the viscosity of the filtrate was analyzed. Moreover, the molecular weight of the CS sample was estimated as described by Wang et al. [26]. The water and fat binding capacity of cCS and sCS were studied where the sample was weighed and mixed into 10 mL of water or corn oil for water and fat absorption respectively. Further, the solution was centrifuged for 30 min (3500 rpm) at 37°C and vortexed every 10 min. Further, the pellet was weighed, and the binding capacity was estimated according to [24]. Furthermore, to determine the EE%, the nanoparticles were dissolved in water and centrifuged separately at 30,000 rpm at 10°C for 30 min. The supernatant was used to calculate the free amount of BSA, which was determined by UV-Vis spectroscopy at 595 nm and EE% was estimated.

Release study of BSA from BSA-CSNPs in vitro

An in vitro release study was performed using a dialysis membrane to study the effect of sCS and BSA concentration on the release of BSA from prepared nanoparticles [27]. Briefly, BSA-CSNPs were prepared using different concentrations of sCS and BSA (3, 2.5, 2, 1.5, and 1 mg/mL). These nanoparticles were dissolved in 3 mL of phosphate buffer saline (PBS) and were kept in the dialysis membrane, which was further incubated in a beaker containing 50 mL of PBS with pH 7.4. The beaker was shaken constantly at 37°C and samples were obtained at 1 h intervals from the beaker for protein estimation using the Bradford assay, whereas an equal amount of buffer was added to the beaker to maintain the volume.

Cell culture and cytotoxicity studies

The biocompatibility assay was performed on L929 cell lines, cultured in DMEM media with 10% FBS. Effects of different concentrations of cCS, sCS as well as BSA-cCSNPs and BSA-sCSNPs were tested for cell cytotoxicity at 24 h using MTT assay as described by Balde et al., [28]. Briefly, cells were seeded in 96 well plates with a cell density of 2 × 10^3 cells/well for 24 h. Further, cells were treated with different concentrations of CS and prepared nanoparticle formulations (5-100 μM) and incubated for 24 h. Furthermore, media was discarded, and cells were washed with 1X PBS. 50 μl of MTT (5 mg/ml) was added and incubated for 4 h. 100 μl of DMSO was added/well and

formazan crystals were dissolved uniformly on the plate shaker. Untreated cells served as a control. Absorbance was recorded at 570 nm to calculate the cell viability (%).

Statistical analysis

All numerical data are presented as mean SD and analyzed with the statistical software package SPSS 12.0 (SPSS Inc, Chicago, IL, USA), with groups compared using one-way ANOVA and the least significant difference test.

RESULTS

Proximate composition

The amount of protein in crude squilla shells was estimated to be $22.66 \pm 1.52\%$ while carbohydrate content was obtained as $12.95 \pm 0.46\%$. Moreover, the ash and moisture content of squilla shells was estimated as mentioned in Table 1. Further, protein and ash content analysis after deproteinization and demineralization step revealed that protein content decreased from $22.66 \pm 1.52\%$ to $0.42 \pm 0.31\%$ and ash content reduced from $38.03 \pm 0.62\%$ to $0.57 \pm 0.13\%$, respectively.

Table 1. Proximate composition analysis of crude squilla shell and processed squilla shell powder after deproteinization as well as demineralization.

	Protein (%)	Ash (%)
Crude Squilla shell powder	22.66 ± 1.52	38.03 ± 0.62
Processed powder (After deproteinization)	0.80 ± 0.21	36.14 ± 1.62
Processed powder (After demineralization)	0.42 ± 0.31	0.57 ± 0.13

Functionality and crystallinity peak analysis of CS and BSA-CSNPs

The FTIR spectrum of cCS showed a sharp peak at 3417.3 cm^{-1} attributed to surface stretching vibrations of O-H and N-H groups. The characteristic peaks at 2916.6 cm^{-1}, 1643.9 cm^{-1}, 1151.2 cm^{-1} are due to the stretching vibration of aliphatic C-H, amide I (-NH deformation of NaHCO3), and C-O-C bonds respectively. The purified CS extracted from squilla showed peaks at 3429.9 cm^{-1}, 2921.9 cm^{-1}, 1642.9 cm^{-1}, and 1084.2 cm^{-1} which are similar to cCS as shown in Figure 1. Similarly, shifting was also observed in the IR spectrum of sCS and BSA-sCSNPs from 3430 cm^{-1} to 3417.9 cm^{-1} and from 1642.8 cm^{-1} to 1634.2 cm^{-1}, which may be due to ionic interaction and cross-linking of polymer CS with TPP and the protein with the successful conversion of CS into nanospheres. Moreover, the absence of a characteristic peak at 1340 cm^{-1} in BSA-sCSNPs is due to reduction in amide-III linkage which can be correlated with the interaction of BSA with the amino group of the polymer while the same was seen with a very less intense peak in BSA-cCSNPs.

In XRD crystallography, diffraction patterns of cCS and sCS were analyzed. Crystalline peaks are mainly used to estimate the presence of mineral, pigment content, and the physical nature of the sample. The spectrum of cCS showed a characteristic peak at 9.84° and 20.06° as illustrated in Figure 2a, which is attributed to the presence of free amino groups and formation of inter and intra-molecular hydrogen bonds [29]. Characteristic peaks at 9.30° and 20.94° were observed for purified sCS which were similar to the cCS

as shown in Figure 2b. Furthermore, CrI for cCS and sCS was calculated to be 89.25 ± 1.25% and 6.612 ± 1.58% respectively, which is directly proportional to the DD%.
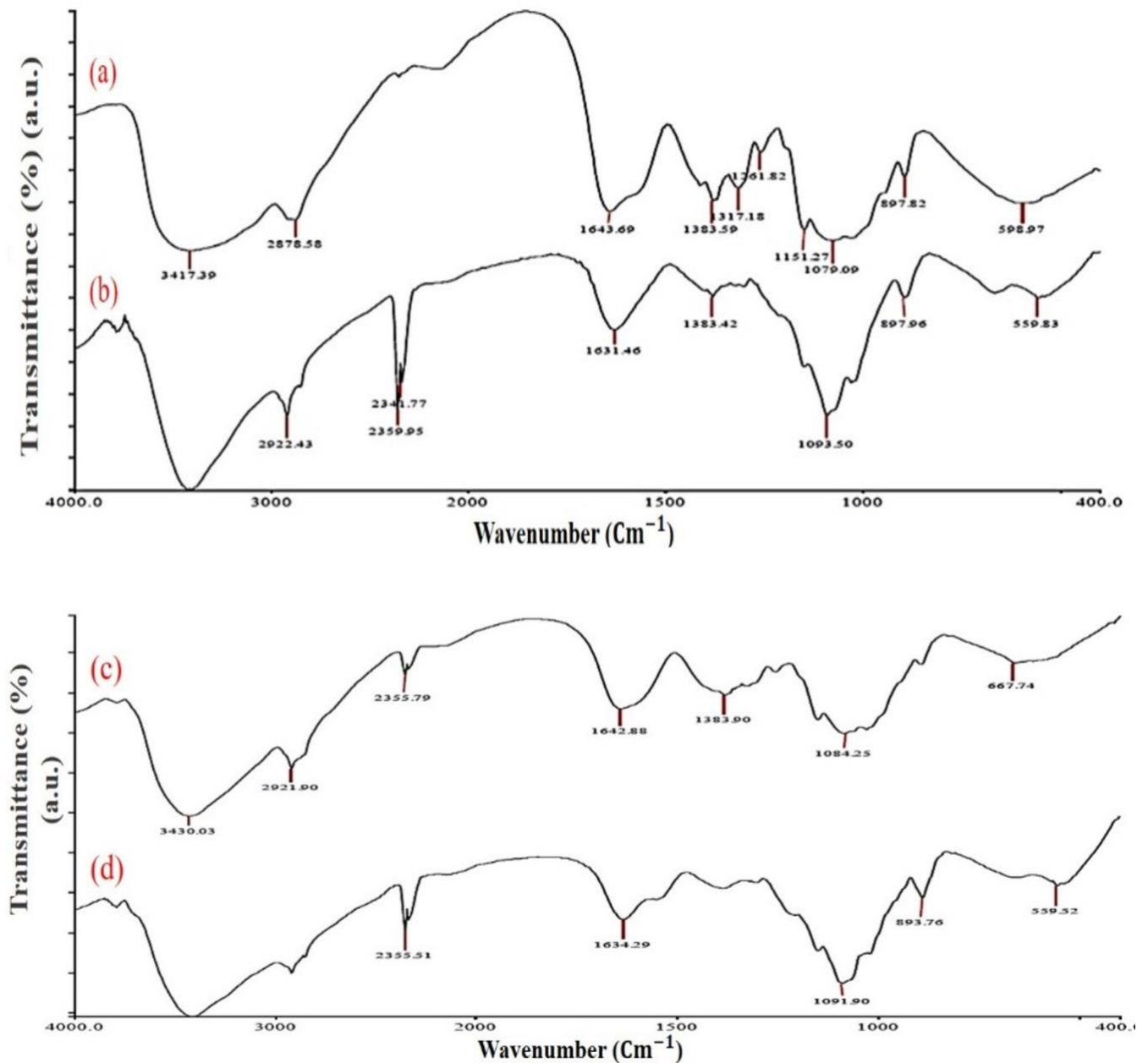
Figure 1. Fourier transform infrared spectra of (a) cCS, (b) BSA-cCSNPs as well as (c) sCS and (d) BSA-sCSNPs, respectively.

Elemental and morphological analysis of CS and BSA-CSNPs

The EDS elemental analysis showed the percentage composition of the atoms present in the compound. Carbon, oxygen, and nitrogen percentage for cCS were found to be 50.23%, 38.24%, and 11.54% whereas sCS was observed to be 49.78%, 39.20%, and 11.01% respectively which were comparable (Figure 2c, d). The extraction process in our study resulted in the successful removal of mineral and pigment content and pure CS was obtained from squills shells. The SEM microimaging of cCS and sCS showed similar morphology were homogenous, smooth, sheet-like surface with amorphous solid particles were observed as reported in Figure 3a, b. Further, SEM analysis of BSA-

cCSNPs showed comparatively large particle sizes ranging from 62 to 452 nm due to the high molecular weight of CS leading to increased agglomeration. Moreover, DD% also affects the binding of the TPP anions with the CS particles. Furthermore, BSA-sCSNPs depicted a distinct spherical shape with particle size range from 60 nm to 195 nm due to low molecular weight and more binding efficiency of CS with BSA with increased binding surface area availability (Figure 3c, d).
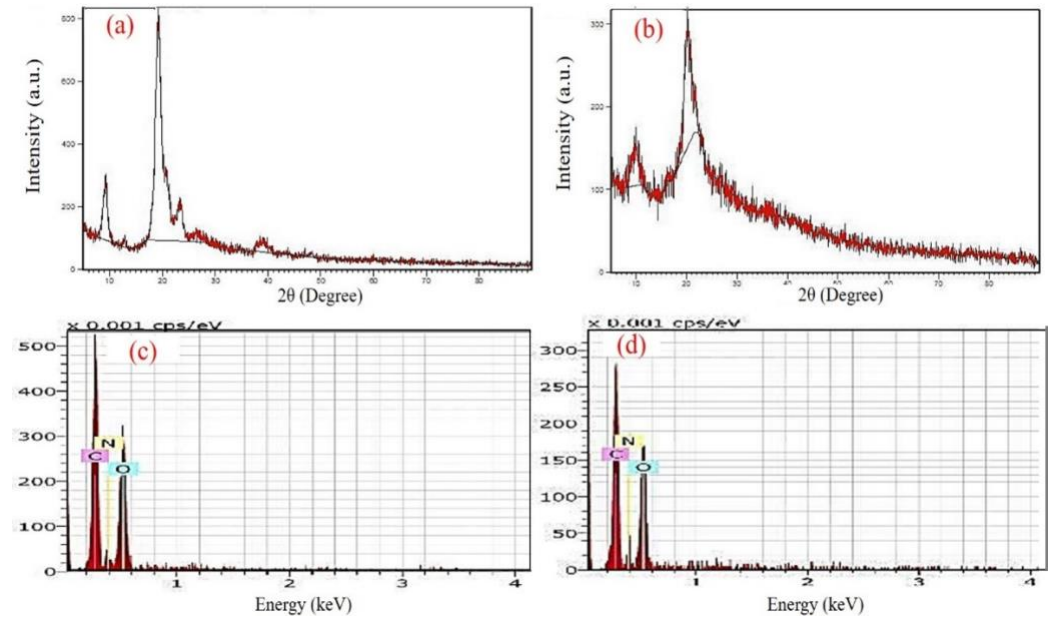
Figure 2. X-ray powder diffraction patterns of (a) cCS, (b) sCS and elemental analysis of (c) cCS, (d) sCS, respectively.
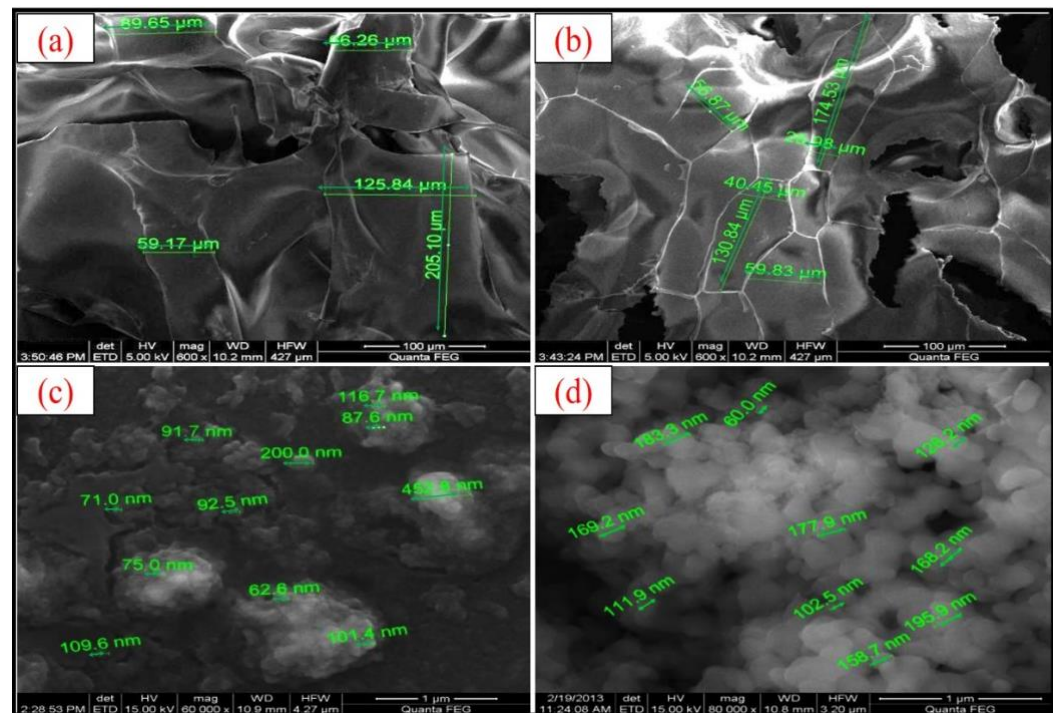
Figure 3. Scanning electron micrograph of (a) cCS, (b) sCS, (c) BSA-cCSNPs and (d) BSA-sCSNPs, respectively.

Physicochemical characteristics of CS and BSA-CSNPs

The physicochemical characteristics of sCS were determined and compared with cCS. The DD% was estimated to be 75% for purified sCS, calculated using the FTIR spectrum. The DD% primarily depends on the process of deacetylation performed for the conversion of chitin to CS where acetyl groups are removed, and free amino groups are exposed. Moreover, the DD% of cCS was found to be 89%. Further, the intrinsic viscosity of squilla and cCS was estimated to be 1.31 ± 0.3 dl/g and 5.89 ± 0.8 dl/g, whereas the molecular weight was estimated to be 50.18 ± 16.8 kDa and 363.92 ± 16.4 kDa respectively. Moreover, the WBC and FBC of sCS were observed to be 548 ± 11.7% and 369 ± 19.9% respectively which are comparable to the capacity of cCS as shown in Table 2. Further, the average particle size obtained for BSA-cCSNPs was 62-452 nm which was larger than the BSA-sCSNPs (60-195 nm) as shown in Figure 4 (a, b). Zeta potential for BSA-sCSNPs and c-BSA-CSNPs was calculated as +48.05 ± 1.87 mV and + 35.05 ± 1.42 mV while the polydispersity index as 0.42 ± 0.023 and 0.26 ± 0.058 respectively (Figure 4c, d).
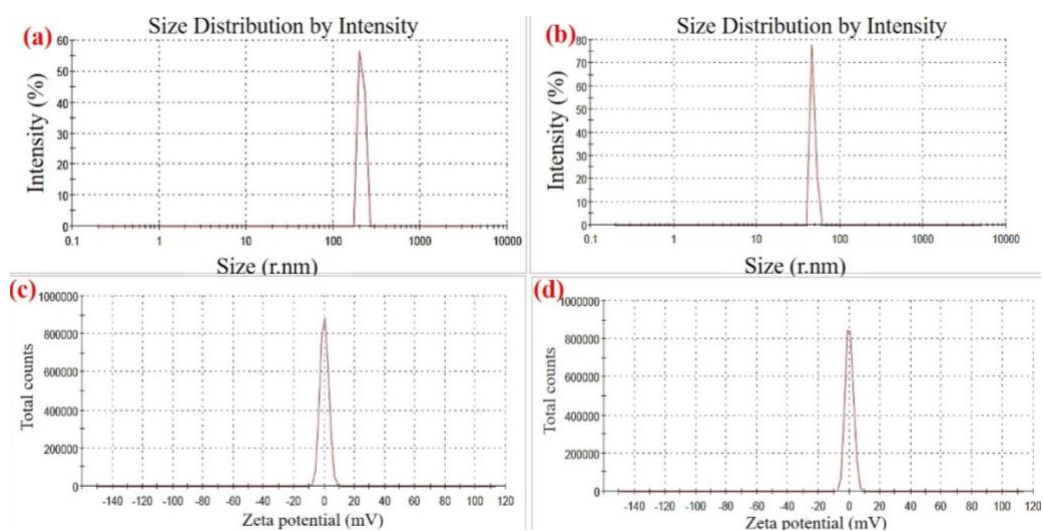
Figure 4. Particle size distribution graph of (a) BSA-cCSNPs, (b) BSA-sCSNPs and zeta potential graph of (c) BSA-cCSNPs, (d) BSA-sCSNPs, respectively.

Table 2. Physicochemical properties of commercialCS (cCS) and squilla CS (sCS).

	Viscosity (dl/g)	Molecular weight (kDa)	DD (%)	FBC (%)	WBC (%)
Commercial CS (cCS)	5.89 ± 0.81	363.92 ± 66.4	89	396 ± 14.22	603 ± 10.42
Squilla CS (sCS)	1.31 ± 0.35	50.18 ± 16.8	75	369 ± 19.92	548 ± 11.71

Whereas DD-Degree of deacetylation; FBC-Fat binding capacity; WBC-Water binding capacity

Nanocarrier efficiency of BSA-CSNPs at different TPP, CS, and BSA concentrations

The EE% of BSA-CSNPs at different concentrations of TPP, CS, and BSA were studied where it was observed that BSA-CSNPs had the highest EE% of 48.75 ± 1.48% and 78.1 ± 3.28% at 1 mg/mL TPP concentration for both BSA-cCSNPs and BSA-sCSNPs respectively. Moreover, the EE% of BSA-sCSNPs reduced from 78.1 ± 3.21% at 1 mg/mL to 48.3 ± 2.15% at 1.5 mg/mL TPP concentration. Similarly, the BSA-cCSNPs also showed similar variations although the EE% range was less than sCS nanoparticles. Further, the effect of BSA concentration on nanocarrier efficiency of BSA-CSNPs was studied at different BSA concentrations (1-3 mg/mL) and constant CS and TPP

concentration of 1 mg/mL which resulted that 1 mg/mL BSA concentration had maximum EE% of 50.2 ± 2.15 and 76.5 ± 3.02% for both BSA-cCSNPs and BSA-sCSNPs respectively as shown in Figure 5a. Furthermore, the EE% decreased significantly with increasing concentration of BSA. Furthermore, CS used for the synthesis of BSA-CSNPs also affected in a similar way where the EE% was found comparatively highest around 50.3 ± 2.96% and 75.6 ± 1.84% at 1 mg/mL cCS and sCS concentration respectively as shown in Figure 5b. Further increase in BSA and CS concentrations reduced EE% in the range of 10-20%. When the CS concentration was increased beyond 3 mg/mL firstly opalescent suspension was detected which dispersed immediately due to the improper agglomeration of CS and TPP molecules. From this study, it was confirmed that for the ionic gelation to take place effectively the CS and BSA concentrations needed to be between 1-3 mg/mL while TPP concentration of 1 mg/mL showed maximum gelation efficiency as illustrated in Figure 5c. Moreover, sCS which had a molecular weight of 50.18 ± 16.8 kDa showed higher EE% as compared to cCS with a molecular weight of 363.92 ± 66.4 kDa. Further, it can also be deduced that the higher the viscosity of CS, the greater number of free amino groups will be present which restricts the interaction of CS with TPP molecules [30].
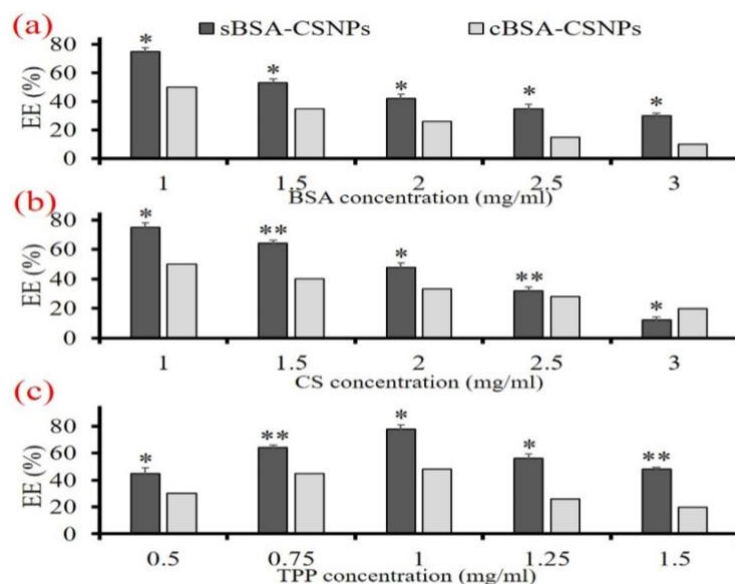
Figure 5. Effect of (a) Bovine serum albumin (BSA) concentration on encapsulation efficiency (EE%) of BSA encapsulated commercial chitosan nanoparticles (BSA-cCSNPs) and BSA encapsulated squilla chitosan nanoparticles (BSA-sCSNPs) where chitosan (CS) and tripolyphosphate (TPP) are 1 mg/mL. (b) CS concentration on EE% of BSA-cCSNPs and BSA-sCSNPs where TPP and BSA are 1 mg/mL. (c) TPP concentration on EE% of BSA-cCSNPs and BSA-sCSNPs where BSA and CS are 1 mg/mL, respectively and mean ± SD, n=3, *p < 0.05, **p <0.01.

Release study of BSA from BSA-CSNPs *in vitro* at different CS and BSA concentrations

In vitro release study of BSA-cCSNPs as well as BSA-sCSNPs illustrated different release rates of BSA at different concentrations of CS and BSA (1-3 mg/mL). As shown in Figure 6 (a and b), the maximum release of BSA from BSA-cCSNPs was found to elevate till 6th h (42.5 ± 2.41%) for 1 mg/mL concentration which subsequently became persistent while the release of BSA from BSA-sCSNPs at a similar concentration was found to be maximum till 16th h around 85.4 ± 2.15%. Further, at 3 mg/mL the cumulative release was reduced although the rate of release consistently increased.

Moreover, it was also observed that the release rate of BSA decreased with an increase in BSA concentration from 1 to 3 mg/mL and the highest release was seen at 1 mg/mL around 81.2 ± 1.18% and 63.6 ± 2.52% for BSA-sCSNPs and BSA-cCSNPs respectively (Figure 6c, d).
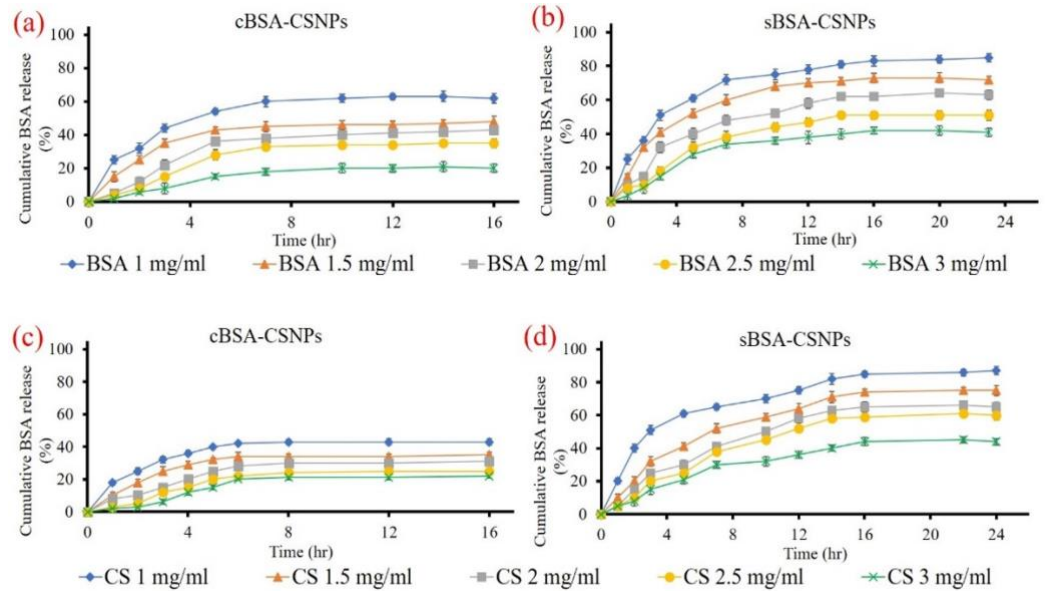
Figure 6. Effect of different chitosan (CS) and bovine serum albumin (BSA) concentrations on cumulative BSA release from (a-c) BSA encapsulated commercial chitosan nanoparticles (BSA-cCSNPs) and (b-d) BSA encapsulated squilla chitosan nanoparticles (BSA-sCSNPs) respectively where mean ± SD, n=3 and *p< 0.05.
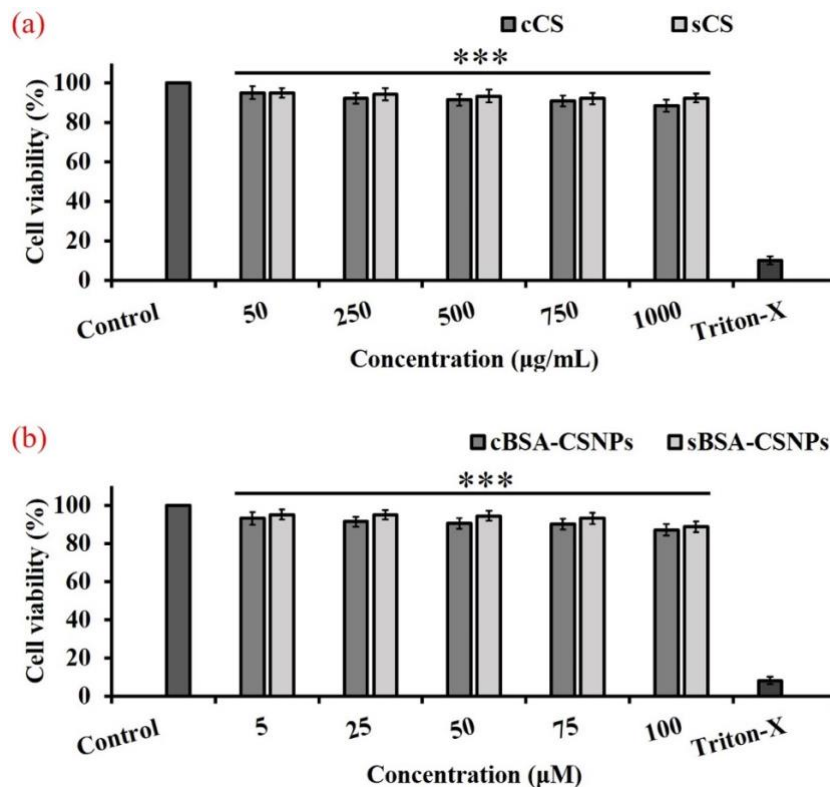
Figure 7. Effect of (a) commercial chitosan (cCS), squilla chitosan (sCS) and(b) BSA encapsulated cCS nanoparticles (BSA-cCSNPs), BSA encapsulated sCS nanoparticles (BSA-sCSNPs) on the viability of L929 cells where mean ± SD, n=3 and ***p < 0.001. Untreated and Triton-X treated cells are considered as control and negative control, respectively.

Effects of nanoparticles on cell viability

As illustrated in Figure 7 (a), sCS showed increased cell viability as compared to cCS. Cell viability was observed to be above 90% at 750 µg/ml cCS and 1000 µg/ml sCS concentration. Similarly, nanoparticle formulations containing different concentrations of BSA were also studied for their cytotoxic effects. It was observed that, BSA-sCSNPs showed increased cell viability at higher concentrations when compared to BSA-cCSNPs. At 75 µM, BSA-cCSNPs and BSA-sCSNPs showed cell viability of 90.11 ± 2.85 % and 93.11 ± 2.51 %, respectively (Figure 7b).

DISCUSSION

Marine crustaceans are widely used for the isolation of bioactive materials such as CS, alginate, peptides, and proteins, which have played a vital role in pharmaceutical, nutraceutical, as well as biomedical applications [28]. Squilla and other crustaceans such as crabs are rich in proteins and hence globally used as a seafood delicacy. Moreover, the shells also contain certain pigments such as astaxanthins, which provide them their colour, whereas removal of these pigments produces white high-value CS, which is also dependent on the processing methods applied [31]. To extract low molecular weight CS, shells are treated by a chemical method which removes unwanted proteins and minerals from them. Further, to study the functional and physicochemical relationship of extracted CS, characterization was performed using FTIR, XRD, and SEM, which showed that our CS was similar to cCS physiochemically. In our study, it was also revealed that the BSA protein was bound to the free amino groups of sCS, present at the nanoparticle surface. While cCS showed low binding with BSA. This may be due to the high molecular weight and DD% of the cCS leading to reduced surface area availability for protein interaction. Similar spectra were reported by Shanmugam et al. [32] for CS and phosphorylated CS derived from *Sepia kobiensis* cuttlebone, showing high anti-bacterial activity. Moreover, Kumari et al. [33] also observed similar functional and crystallinity peaks for fish, crab, and shrimp shell derived CS.

CS is a biodegradable polymer that mostly consists of only C, H, O, and N in its structure due to which the degradation becomes easy in the optimal environment and mildly acidic conditions lead to the removal of all mineral content from the sample [34]. Hence, the extracted CS should not have heavy metal content for its non-cytotoxic effects. The sCS did not have any heavy metal presence such as Mn, Fe or Cd. Physicochemical property investigations of CS are important which reveal the ability of CS to bind to water as well as fats. The same helps in understanding the potential of using extracted CS in food and nutraceutical applications. Similar to our study, Kucukgulmez et al. [35] reported WBC and FBC of CS obtained from *Metapenaeus stebbingi* shells which were observed to be 712.99% and 531.15% respectively. It can also be stated that WBC changes with the change in the method of extraction processes of CS such as deproteinization before demineralization reduces the WBC while the decolorization step before demineralization increases the FBC due to the remains of certain hydrophilic groups into the molecular composition. WBC and FBC are directly related to the viscosity of the polymeric materials. The decrease in viscosity leads to a decrease in FBC and WBC. Moreover, less viscous polymers attain a lower molecular weight. Hence, less molecular weight CS has less binding capacities. Moreover, The WBC and FBC are directly affected by the change in DD% of CS. As the DD% increases, the WBC and FBC also increase, majorly due to the removal of acetyl groups from the polymeric structure during the preparation steps and change in crystallinity. Moreover,

maintaining zeta potential is an important process to inhibit the aggregation of nanoparticles which is mainly affected by pH, ionic strength, temperature, and most importantly van der Waals interparticle hold [36]. The increase in zeta potential may be due to a greater number of free NH3+ charges present on the nanoparticles which may lead to more protein binding to the surface of the nanocarrier system [37]. Further, studies have shown that increase in BSA concentration increases the pH of the solution and hence the ionization of amino groups decreases. This results in the prolonged gelation process and ionic interaction of CS and TPP molecules due to which the EE% of nanocarriers is reduced as the BSA gets very tightly bonded to the inner core and takes more time to diffuse out of the nanoparticle system. Molecular weight is an important parameter to determine the efficiency of nanoparticle formation as molecular weight spread the polymeric length of CS in solution which affects the protein interaction and encapsulation as well [38].

Hence, in our study, it is shown that nanoparticles prepared from sCS with lower DD% as compared to cCS showed the highest EE% at 1 mg/mL of BSA, CS, and TPP concentration. Similarly, in previous studies by Balde et al. [24], CS extracted from squilla *Carinosquilla multivariate* showed a molecular weight of 54 kDa while the EE% of diclofenac loaded nanoparticles was found to be 40.33 ± 1.85% at CS: TPP ratio of 5:2. Also, our study revealed that the cCS-based nanoparticles are observed to show the reduced release of protein due to high molecular weight and DD% which leads to less surface area and amino groups available for the protein to bind. While low molecular weight CS provided lower viscosity, which does not allow the formation of highly dense TPP-CS matrix leading to higher swelling ability. Moreover, a decrease in the release rate at higher concentrations can be attributed because of inefficient agglomeration of CS with TPP, and BSA protein. The interaction of BSA with CS plays an important role in the release rate as recent studies suggest that BSA binds with CS through non-covalently linked complexes and also depict certain conformational changes at different physiological pH environment which may also affect particle size and zeta potential of nanoparticles [39]. It can also be compared with the EE% of nanoparticles where BSA-sCSNPs with high EE% showed increased release of BSA in a sustained manner as compared to BSA-cCSNPs. Hence, nanoparticles with 1 mg/mL concentration of sCS, BSA, and TPP was optimum for high EE% and prolonged release of protein.

CS is a biocompatible polymer which has shown least toxic effects for various cell lines investigated previously. Recently, Chaudhry et al. [40], studied the cytotoxic effects of different CS and CS oligosaccharide concentrations on MCF-7, HepG2, 3T3 and HeLa cell lines. It was observed that CS showed lower cytotoxic effects, although MCF-7 cells developed higher toxicity compared to other cells at 1 mg/ml. According to Dev et al. [41], 5-fluorouracil encapsulated nanoparticles were observed to be non-toxic for L929 fibroblast cells. Similar to our studies, Yadav and Yadav, [42] also studied the effects of BSA-CSNPs on A549 cell line, where the BSA loaded nanoparticles were biocompatible and showed low cytotoxic effects. Hence, marine waste extracted CS can effectively be used for the extraction of low molecular weight CS and develop uniform nanoparticle formulation by the ionic gelation method. These nanoparticles can act as a potent protein delivery carrier with minimal cytotoxic effects, which can be used as a therapeutic to treat various disease and deliver protein to the targeted site.

CONCLUSION

In the present work, CS was successfully extracted from the exoskeleton of a squilla (*H. annandalei),* displaying lower molecular weight and effective binding capacities than cCS. Moreover, BSA entrapped nanoparticles prepared from squilla as well as cCS through TPP cross-linking exhibited desirable functional and morphological characteristics. When compared with BSA-cCSNPs, the BSA-sCSNPs were found to be more effective in protein encapsulation with a sustained-release rate at 1 mg/mL CS, BSA, and TPP concentrations. Further, the extracted sCS as well as BSA-sCSNPs showed no cytotoxicity on L929 cells when compared to cCS and BSA-cCSNPs at higher concentrations. Hence, these biocompatible and cost-effective nanoparticles can be used in various pharmaceutical applications for the controlled release of proteins to the targeted site.

ACKNOWLEDGMENT

AUTHOR CONTRIBUTIONS

Formal analysis and methodology: Bhavika Waghela. Interpretation of data and drafting the manuscript: Akshad Balde. Conceptualization and supervision: Nazeer Rasool Abdul.

CONFLICTS OF INTEREST

There is no conflict of interest among the authors.

REFERENCES

[1]   Bandara S, Du H, Carson L, Bradford D, Kommalapati R. Agricultural and biomedical applications of chitosan-based nanomaterials. Nanomaterials 2020; 10:1903.

[2]   Singh AP, Biswas A, Shukla A, Maiti P. Targeted therapy in chronic diseases using nanomaterial-based drug delivery vehicles. Signal Transduct Target Ther 2019; 4:33.

[3]   Banerjee A, Das D, Andler R, Bandopadhyay R. Green synthesis of silver nanoparticles using exopolysaccharides produced by Bacillus anthracis PFAB2 and its biocidal property. J Polym Environ 2021; 29:2701–9.

[4]   Stella B, Andreana I, Zonari D, Arpicco S. Pentamidine-loaded lipid and polymer nanocarriers as tunable anticancer drug delivery systems. J Pharm Sci 2020; 109:1297–302.

[5]   Taghipour-Sabzevar V, Sharifi T, Bagheri-Khoulenjani S, Goodarzi V, Kooshki H, Halabian R, et al. Targeted delivery of a short antimicrobial peptide against CD44-overexpressing tumor cells using hyaluronic acid-coated chitosan nanoparticles: An in vitro study. J Nanopart Res 2020;22.

[6]   Vijayan S, Divya K, Jisha MS. In vitro anticancer evaluation of chitosan/biogenic silver nanoparticle conjugate on Si Ha and MDA MB cell lines. ApplNanosci2020; 10:715–28.

[7]   Hong S, Choi DW, Kim HN, Park CG, Lee W, Park HH. Protein-based nanoparticles as drug delivery systems. Pharmaceutics 2020; 12:604.

[8]   Scaletti F, Hardie J, Lee Y-W, Luther DC, Ray M, Rotello VM. Protein delivery into cells using inorganic nanoparticle–protein supramolecular assemblies. Chem Soc Rev 2018; 47:3421–32.

[9]   Tanganini IC, Shirahigue LD, Altenhofen da Silva M, Francisco KR, Ceccato-Antonini SR. Bioprocessing of shrimp wastes to obtain chitosan and its antimicrobial potential in the context of ethanolic fermentation against bacterial contamination. 3 Biotech 2020; 10:135.

[10] Narayanasamy A, Balde A, Raghavender P, Shashanth D, Abraham J, Joshi I, et al. Isolation of marine crab (*Charybdis natator*) leg muscle peptide and its anti-inflammatory effects on macrophage cells. Biocatal Agric Biotechnol2020; 25:101577.

[11] Odeleye T, White WL, Lu J. Extraction techniques and potential health benefits of bioactive compounds from marine molluscs: a review. Food Funct2019; 10:2278–89.

[12] Venkatesan J, Anil S, Kim S-K, Shim M. Marine Fish Proteins and Peptides for Cosmeceuticals: A Review. Mar Drugs 2017; 15:143.

[13] Gaspar-Pintiliescu A, Stefan LM, Anton ED, Berger D, Matei C, Negreanu-Pirjol T, et al. Physicochemical and biological properties of gelatin extracted from marine snail *Rapana venosa*. Mar Drugs 2019; 17:589.

[14] Metin C, Alparslan Y, Baygar T, Baygar T. Physicochemical, microstructural and thermal characterization of chitosan from blue crab shell waste and its bioactivity characteristics. J Polym Environ 2019; 27:2552–61.

[15] Ramanathan G, Singaravelu S, Muthukumar T, Thyagarajan S, Rathore HS, Sivagnanam UT, et al. Fabrication of *Arothron stellatus* skin collagen film incorporated with *Coccinia grandis* as a durable wound construct. Int J Polym Mater 2017; 66:558–68.

[16] Mohammed M, Syeda J, Wasan K, Wasan E. An overview of chitosan nanoparticles and its application in non-parenteral drug delivery. Pharmaceutics 2017; 9:53.

[17] Sabnis S, Block LH. Chitosan as an enabling excipient for drug delivery systems: I. Molecular modifications. Int J Biol Macromol2000; 27:181–6.

[18] Antelo LT, Lopes C, Franco-Uría A, Alonso AA. Fish discards management: pollution levels and best available removal techniques. Mar Pollut Bull 2012; 64:1277–90.

[19] Zhang D, Zuo X, Wang P, Gao W, Pan L. Influence of chitosan modification on self-assembly behavior of Fe3O4 nanoparticles. ApplNanosci2021; 11:21–7.

[20] Lowry OH, Rosebrough NJ, Farr AL, Randall RJ. Protein measurement with the Folin phenol reagent. J Biol Chem 1951; 193:265–75.

[21] Albalasmeh AA, Berhe AA, Ghezzehei TA. A new method for rapid determination of carbohydrate and total carbon concentrations using UV spectrophotometry. CarbohydrPolym2013; 97:253–61.

[22] Rao S, Nyein A, Trung S, Stevens T. Optimum parameters for production of chitin and chitosan from squilla (*S. empusa*). J ApplPolym Sci 2007; 103:3694–700.

[23] Yang W, Fu J, Wang T, He N. Chitosan/sodium tripolyphosphate nanoparticles: preparation, characterization and application as drug carrier. J Biomed Nanotechnol2009; 5:591–5.

[24] Balde A, Hasan A, Joshi I, Nazeer RA. Preparation and optimization of chitosan nanoparticles from discarded squilla (*Carinosquilla multicarinata*) shells for the delivery of anti-inflammatory drug: Diclofenac. J Air Waste Manag Assoc 2020; 70:1227–35.

[25] Fernández-Urrusuno R, Calvo P, Remuñán-López C, Vila-Jato JL, Alonso MJ. Enhancement of nasal absorption of insulin using chitosan nanoparticles. Pharm Res 1999; 16:1576–81.

[26] Wang W, Bo S, Li S, Qin W. Determination of the Mark-Houwink equation for chitosans with different degrees of deacetylation. Int J Biol Macromol1991; 13:281–5.

[27] Mohammadi Z, Samadi FY, Rahmani S, Mohammadi Z. Chitosan-Raloxifene nanoparticle containing doxorubicin as a new double-effect targeting vehicle for breast cancer therapy. Daru 2020; 28:433–42.

[28] Balde A, Raghavender P, Dasireddy S, Abraham J, Prasad S, Joshi I, et al. Crab pentapeptide and its anti-inflammatory activity on macrophage cells. Int J Pept Res Ther2021; 27:2595–605.

[29] Aranaz I, Mengibar M, Harris R, Panos I, Miralles B, Acosta N, et al. Functional characterization of chitin and chitosan. Curr Chem Biol 2009; 3:203–30.

[30] Al-Nemrawi NK, Alsharif S, Dave RH. Preparation of chitosan-TPP nanoparticles: the influence of chitosan polymeric properties and formulation variables. Int J Appl Pharm 2018; 10:60–5.

[31] Sarbon NM, Sandanamsamy S, Kamaruzaman SFS, Ahmad F. Chitosan extracted from mud crab (*Scylla olivicea*) shells: physicochemical and antioxidant properties. J Food Sci Technol 2015; 52:4266–75.

[32] Shanmugam A, Kathiresan K, Nayak L. Preparation, characterization and antibacterial activity of chitosan and phosphorylated chitosan from cuttlebone of *Sepia kobiensis* (Hoyle, 1885). Biotechnol Rep (Amst) 2016; 9:25–30.

[33] Kumari S, Kumar Annamareddy SH, Abanti S, Kumar Rath P. Physicochemical properties and characterization of chitosan synthesized from fish scales, crab and shrimp shells. Int J Biol Macromol2017; 104:1697–705.

[34] Eddya M, Tbib B, El-Hami K. A comparison of chitosan properties after extraction from shrimp shells by diluted and concentrated acids. Heliyon 2020;6: e03486.

[35] Kucukgulmez A, Celik M, Yanar Y, Sen D, Polat H, Kadak AE. Physicochemical characterization of chitosan extracted from *Metapenaeus stebbingi* shells. Food Chem 2011; 126:1144–8.

[36] Chang S-H, Lin H-TV, Wu G-J, Tsai GJ. pH Effects on solubility, zeta potential, and correlation between antibacterial activity and molecular weight of chitosan. CarbohydrPolym2015; 134:74–81.

[37] Sotelo-Boyás ME, Correa-Pacheco ZN, Bautista-Baños S, Corona-Rangel ML. Physicochemical characterization of chitosan nanoparticles and nanocapsules incorporated with lime essential oil and their antibacterial activity against food-borne pathogens. LebensonWiss Technol 2017; 77:15–20.

[38] Dounighi M, Eskandari N, Avadi R, Zolfagharian MR, Sadeghi MM, Rezayat A. Preparation and in vitro characterization of chitosan nanoparticles containing *Mesobuthus eupeus* scorpion venom as an antigen delivery system. J Venomous Anim Toxins Incl Trop Dis 2012; 18:44–52.

[39] Li G, Huang J, Chen T, Wang X, Zhang H, Chen Q. Insight into the interaction between chitosan and bovine serum albumin. CarbohydrPolym2017; 176:75–82.

[40] Chaudhry G-E-S, Thirukanthan CS, NurIslamiah KM, Sung YY, Sifzizul TSM, Effendy AWM. Characterization and cytotoxicity of low-molecular-weight chitosan and chito-oligosaccharides derived from tilapia fish scales. J Adv Pharm Technol Res 2021; 12:373–7.

[41] Dev A, Mohan JC, Sreeja V, Tamura H, Patzke GR, Hussain F, et al. Novel carboxymethyl chitin nanoparticles for cancer drug delivery applications. CarbohydrPolym2010; 79:1073–9.

[42] Yadav P, Yadav AB. Preparation and characterization of BSA as a model protein loaded chitosan nanoparticles for the development of protein-/peptide-based drug delivery system. Futur J Pharm Sci 2021; 7.